First-Pass Radionuclide Angiographic Analysis with Two Regions of Interest to Improve Left Ventricular Ejection Fraction Accuracy

Kim A. Williams, Todd A. Bryant and Linda A. Taillon

Departments of Medicine (Cardiology) and Radiology (Nuclear Medicine), The University of Chicago, Chicago, Illinois

First-pass radionuclide angiographic (FPRNA) analysis, using the standard, single-fixed region of interest (ROI) drawn at end-diastole, often underestimates the left ventricular ejection fraction (LVEF) as determined by other standard techniques. This study examined the hypothesis that correction for the anatomic motion of the aortic valve plane toward the apex during systole, which results in improper inclusion of aortic counts within the single-fixed ROI, using a two-ROI method to compensate for this motion would eliminate this underestimation. **Methods:** In 70 patients who underwent FPRNA and planar gated equilibrium radionuclide angiography (GERNA) on the same day, Fourier transform phase and amplitude images were used to generate functional maps of the aorta and the left ventricle on the FPRNA representative cycle. The region of low amplitude between the aorta and left ventricle, which corresponds to the degree of aortic valve plane motion, was used to guide the manual placement of two ROIs. The first was over the left ventricle at the end-diastole including the aortic valve plane area, and the second was a smaller end-systolic ROI drawn over the first ROI, excluding the valve plane area. **Results:** Both the fixed- and dual-ROI FPRNA methods had excellent correlation with GERNA (r = 0.92 and 0.91, respectively). The mean FPRNA LVEF using a fixed ROI (45%± 14%) was significantly lower than GERNA (51% ± 15%, p < 0.001), but the mean LVEF calculated from the dual-ROI (51% ± 14%) was essentially identical to those obtained with GERNA. The method of manual placement of the two ROIs had extremely high levels of inter- and intraobserver reproducibility (r = 0.98 and 0.99, respectively). **Conclusion:** Despite good correlation, the standard, fixed-ROI method of FPRNA analysis systematically underestimates the LVEFs of GERNA. This problem can be eliminated by taking into account valve plane motion during the cardiac cycle by using Fourier-guided, dual-ROI analysis on FPRNA. These differences in methods and results should be considered when substituting or comparing LVEFs derived from these techniques.

Key Words: dual region of interest; Fourier transformation; amplitude image

The noninvasive assessment of resting left ventricular (LV) performance has become an integral part of the evaluation of patients with known or suspected cardiac disease, having important diagnostic, therapeutic and prognostic significance (1–10). In particular, the exercise first-pass radionuclide angiographic (FPRNA) left ventricular ejection fraction (LVEF) has greater prognostic value in patients with ischemic heart disease than many other clinical, noninvasive and invasively-derived variables (5–9).

An exercise LVEF of 0.50 (50%) has been detected as the inflection point below which patients with coronary artery disease demonstrate a probability of cardiac death that increases as the LVEF decreases (7). However, the direct applicability of these numerical data when the LVEF is obtained with other protocols or techniques, such as the more widely used multiple-gated acquisition (MUGA) or gated equilibrium radionuclide angiographic (GERNA) technique, is uncertain.

There has been renewed interest in FPRNA, at least in part, because of the availability of ^{99m}Tc-labeled perfusion tracers that allow simultaneous evaluation of myocardial perfusion and ventricular function (11–22). However, the widespread application of FPRNA has been limited by the need for a high-count rate capable gamma camera, dependence on impeccable bolus technique and the absence of valvular (especially tricuspid) incompetence for data quality (23).

Despite good correlation coefficients between FPRNA and other LVEF techniques (22,24–27), it has been reported that FPRNA may underestimate both invasively- and noninvasively-derived EFs by as much as 12% to 25% (22,24–26). One potential reason for this underestimation is the use of a single-fixed region of interest (ROI) drawn at end-diastole, which does not account for valve plane motion (base toward apex) during systole (22,26). This shortening motion of the heart is more pronounced in vigorously contracting ventricles (28–31). If this motion is not considered during LVEF analysis, inclusion of counts from above the aortic valve plane within the LV ROI during systole results in a lower calculated LVEF.

This study was undertaken to examine the degree of underestimation of the standard GERNA LVEFs by FPRNA and to determine if the use of a Fourier transformation guided dual-ROI approach to FPRNA LVEFs could correct this underestimation.

MATERIALS AND METHODS

Patient Population

Resting FPRNA and GERNA were performed on the same day for clinical indications in 70 patients (47 men, 23 women; mean age 56 ± 14 yr). These patients included 31 patients with known ischemic heart disease. Resting regional wall motion abnormalities were present in 45 patients. No patient had valvular heart disease of the severity that would preclude good bolus transit for FPRNA (23). No patient had persistent resting arrhythmias that would interfere with electrocardiogram (ECG) gating.

First-Pass Radionuclide Angiography with a Single-Fixed Region of Interest. After placement of a large bore (14- or 16-gauge) antecubital intravenous line, 1.5 mg of stannous pyrophosphate was mixed with 30 ml of the patient's blood for approximately 60 sec and was then infused. Resting FPRNA was performed after a 10-min delay, to allow further red blood cell uptake of the stannous ion. Technetium-99m-pertechnetate (25–30 mCi), in a volume of less than 1 ml, was given by rapid flushing with at least 30 ml of normal saline through the indwelling catheter. Images were obtained using a single-crystal, high-count rate gamma camera fitted with a high-sensitivity, parallel-hole collimator (Elscint Apex
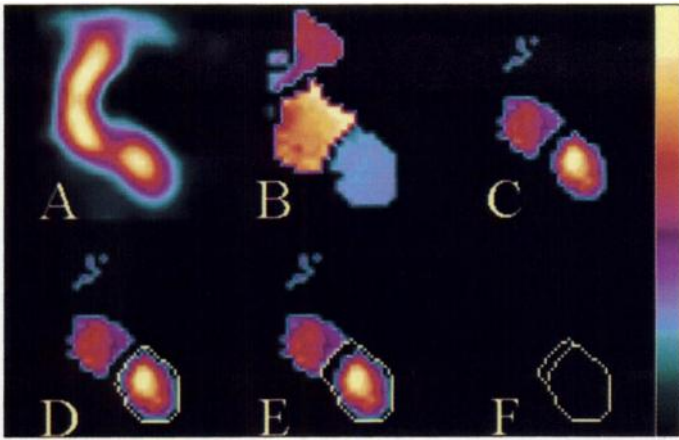
FIGURE 1. Anterior projection first-pass radionuclide angiographic images are shown. (A) Representative cycle end-diastolic frame, (B) Fourier-phase and (C) amplitude are shown. Note presence of amplitude in both left ventricle and aorta, which are easily distinguished by opposite values on phase image and are separated by low-amplitude region. (D) Valve plane of end-systolic region of interest (ROI) is drawn using inferior margin of this amplitude image. (E) End-diastolic ROI is obtained by tracing end-systolic ROI, except for valve plane, which is drawn using upper margin of low amplitude region. (F) These dual ROIs are shown comparatively.

409AG, Hackensack, NJ). Images were acquired in the anterior projection using 25 (± 4) frames per cardiac cycle.

FPRNA data were analyzed using the frame method for LVEF using commercially available Elscint computer software (13,32,33). This software creates a representative LVEF volume curve by summing frames of several (usually 5–10) cardiac cycles, which are aligned by matching their end-diastoles (histogram peaks) and end-systoles (histogram valleys) during the operator-defined levophase of tracer transit. The pulmonary frame background-corrected representative cycle was then interrogated with a fixed ROI to obtain the final first-pass LVEF time-activity curve. This ROI was drawn over the LVEF as defined by a first-harmonic, Fourier transformation phase image that distinguishes clearly the LVEF from the aortic counts (Fig. 1). End-diastole was taken as the first frame of the representative cycle, and end-systole was defined as the frame with the minimum counts in the histogram. The LVEF was taken as the end-diastolic counts minus the end-systolic counts, divided by the background subtracted end-diastolic counts.

First-Pass Analysis with Dual Regions of Interest. As shown in Figure 1, a second ROI (end-diastolic) was derived from a Fourier transformation amplitude image with masking of the lower 10% of image intensity, which extended the ROI in a basal direction, usually 1–3 pixels, up to the amplitude signal of the aortic root. The remainder of this ROI was drawn to match the first ROI (end-systolic). The dual-ROI LVEF was determined as the end-diastolic ROI counts minus the end-systolic ROI counts, divided by the background subtracted end-diastolic ROI counts.

Gated Planar Equilibrium Blood-Pool Image Acquisition and Analysis. ECG-gated planar equilibrium blood-pool images also were acquired using an Elscint Apex-409AG large-field of view gamma camera equipped with a high-resolution collimator. Images for LVEF calculation were obtained in the best-septal (shallow), left-anterior oblique view in 64 × 64-byte mode. Each planar-gated image was acquired for 6–10 min duration, dividing each cardiac cycle into a minimum of 32 frames.

Automated variable ROIs were generated throughout the cardiac cycle using the commercially-available software. This method automatically determines the LV master ROI by Fourier-phase imaging, requiring no operator intervention, followed by the edge detection technique described earlier. An automated periventricular background ROI was adjusted routinely to avoid inclusion of

high-count structures (e.g., spleen, ventricle and descending aorta), which could artifactually increase the LVEF.

Statistical Analysis

Linear regression analysis was performed to determine the product-moment correlation coefficient (r), reflecting the degree of random error, between the LVEFs using the three radionuclide techniques. Statistically significant differences between correlation coefficients were assessed by using a two-tailed Fisher's z transformation (34). The degree of systematic error between these performance indices, as well as their degree of agreement, was assessed using Bland-Altman plots (35,36). This technique plots the mean of the paired observations of the two techniques on the abscissa (x-axis) and the difference between their values on the ordinate (y-axis). The mean difference between the two techniques and 2 s.d. above and below this mean also are shown. This analysis determines the limits and degree of agreement between the values obtained with each technique, the degree of bias of one method to give results that are higher or lower than the other technique and whether or not a relationship exists between the degree of under- or overestimation and the mean value of any two techniques (e.g., greater overestimation at higher test values). Paired Student's t-tests also were performed on these data to determine if the values obtained with any of these techniques were substantially numerically different from the other techniques. These data are presented as mean ± 1 s.d. A p-value of < 0.05 was considered statistically significant.

RESULTS

Comparison of Ejection Fractions

The mean LVEF obtained with FPRNA using the standard-fixed ROI approach was 0.45 ± 0.14, which was significantly lower than that obtained with GERNA (0.51 ± 0.15, p < 0.001 versus FPRNA), a 13% underestimation of GERNA values. Reprocessing the FPRNA data using the dual-ROI approach gave a mean LVEF essentially identical to that of GERNA (0.51 ± 0.14, also p < 0.001 versus FPRNA). Consistent with the presence of other differences between the FPRNA and GERNA (e.g., preload alteration from upright to supine position and the effects of regional wall motion abnormalities on LVEFs obtained from two different projections), there were occasional patients with striking differences between FPRNA and GERNA (Fig. 2). These differences ranged from −0.23 to +0.07 in LVEF; these differences were shifted upward, but not reduced, by the dual-ROI analysis to a range of −0.19 to +0.12 units.

The correlation coefficients between the LVEFs obtained with each of the three techniques were very high (Fig. 2), ranging from 0.91 between GERNA and dual-ROI (z = 18.1) to 0.98 between FPRNA and dual-ROI (z = 42.7). Average versus difference (Bland-Altman) plots demonstrated a significantly greater difference between the single- and dual-region techniques in the higher LVEF range (r = 0.234, p = 0.0478). This observation is consistent with the need for a greater degree of correction for a greater degree of valve plane excursion that occurs with more vigorous systolic contraction.

Reproducibility of Dual Region-of-Interest Ejection Fractions

Since the dual-ROI method is dependent on manual placement of two overlapping ROIs around the LV chamber, differing in only the valve plane, the intra-and interobserver variability of the technique was examined in 21 patients (Fig. 3). There was no significant difference between the LVEFs obtained by two different observers, or between the first and second analysis by the same observer. As shown in Figure 3, both inter- and intraobserver differences were negligible, with
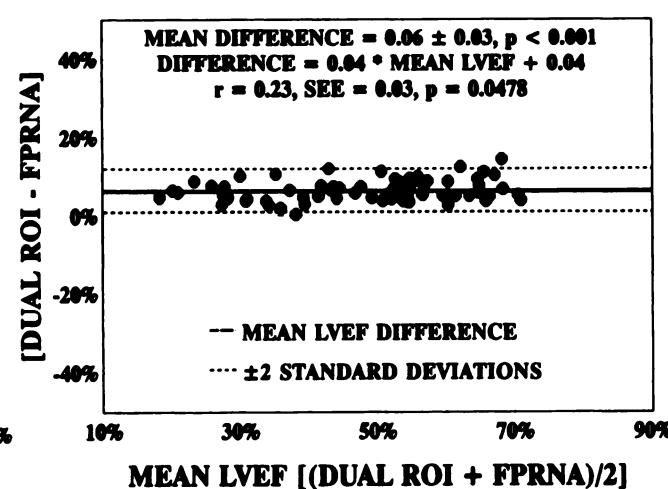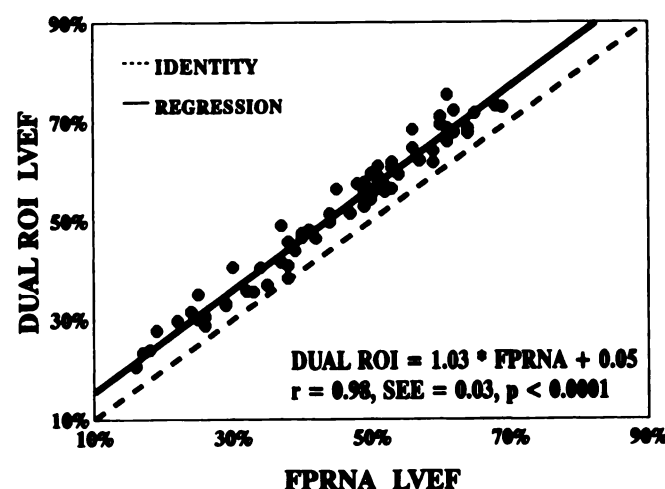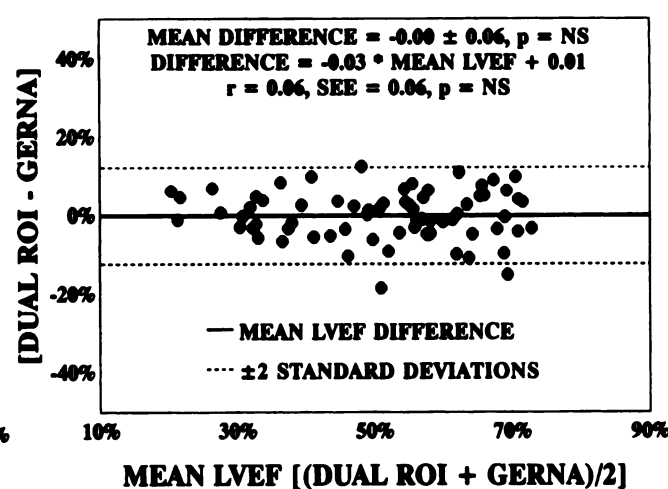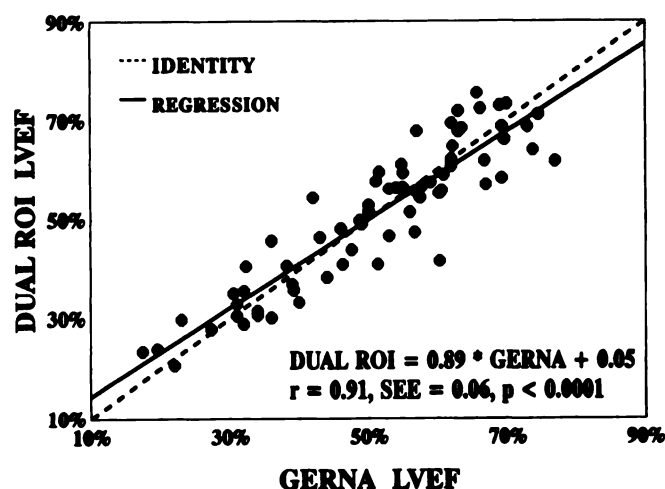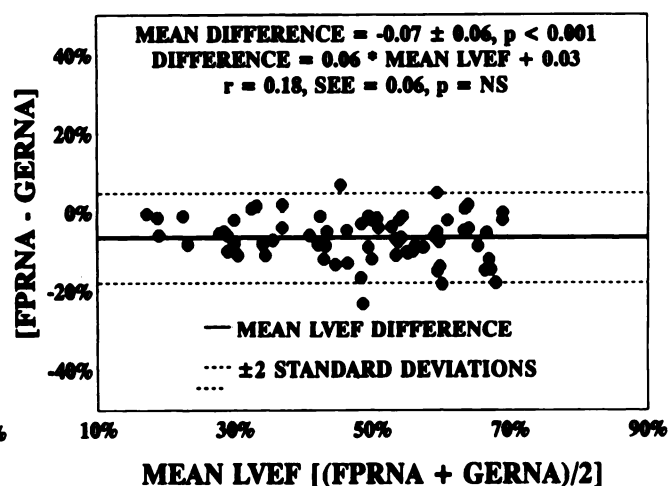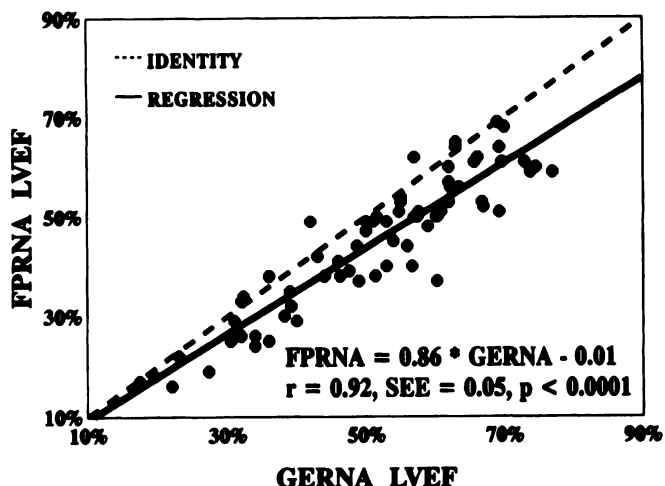
LVEF CORRELATIONS

BLAND-ALTMAN PLOTS

FIGURE 2. Scatter plots (left) and Bland-Altman plots (right) are shown for left ventricular ejection fractions (LVEF) obtained with gated equilibrium radionuclide angiography (GERNA) and first-pass radionuclide angiography (FPRNA) in 70 patients. Excellent correlation coefficients and regression line slope near unity were found between each of three techniques. Significant mean differences were present between values obtained with FPRNA and GERNA and between FPRNA and dual region-of-interest (ROI). On Bland-Altman analysis, there was significantly greater difference between single- and dual-ROI methods at higher LVEF values. SEE = s.e. of y-estimate.

excellent correlation coefficients (0.98 and 0.99, respectively), y-intercepts near 0, and regression line slopes of near unity. No significant bias or correlation between mean values and difference was found on Bland-Altman plots.
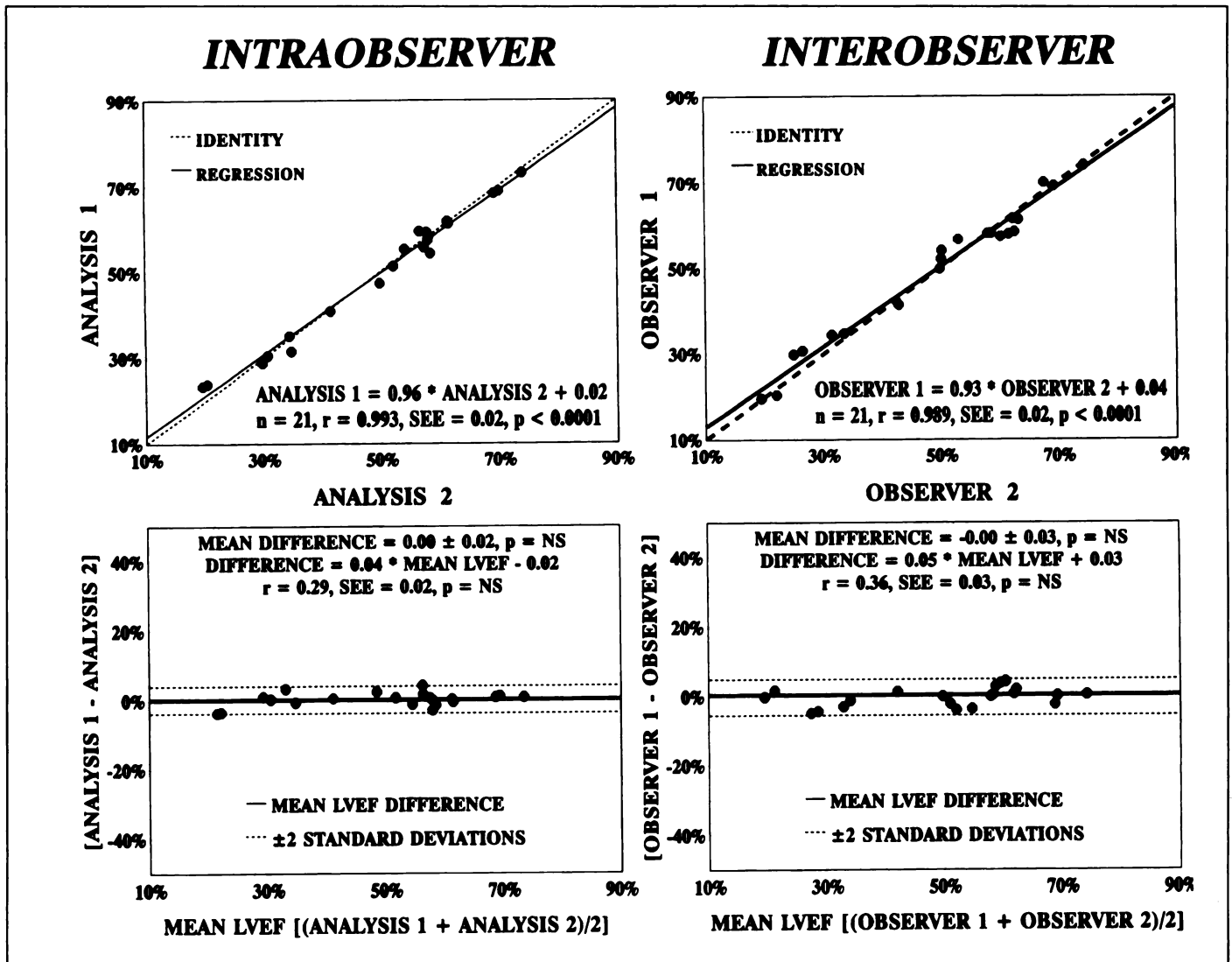
INTRAOBSERVER

ANALYSIS 1 = 0.96 * ANALYSIS 2 + 0.02
n = 21, r = 0.993, SEE = 0.02, p < 0.0001

MEAN DIFFERENCE = 0.00 ± 0.02, p = NS
DIFFERENCE = 0.04 * MEAN LVEF - 0.02
r = 0.29, SEE = 0.02, p = NS

INTEROBSERVER

OBSERVER 1 = 0.93 * OBSERVER 2 + 0.04
n = 21, r = 0.989, SEE = 0.02, p < 0.0001

MEAN DIFFERENCE = -0.00 ± 0.03, p = NS
DIFFERENCE = 0.05 * MEAN LVEF + 0.03
r = 0.36, SEE = 0.03, p = NS

FIGURE 3. Intra-and interobserver variability of dual region-of-interest technique is shown. There was no significant difference between left ventricular ejection fractions obtained by two different observers or between first and second analysis by same observer. No significant bias or correlation between mean values and value differences was found on Bland-Altman plots.

DISCUSSION

The evaluation of LV systolic function has become one of the most common applications of nuclear imaging using FPRNA, planar GERNA and, more recently, gated tomographic perfusion and equilibrium blood-pool imaging. Between these techniques, FPRNA has some distinct advantages. These include the acquisition of data in less than 30 sec, right ventricular function with less overlap of activity in other chambers (23), the use of multiple radiopharmaceuticals including bone, renal and myocardial scintigraphic agents (13), a proven robust measurement of stress ventricular function at true peak exercise, and the presence of a wealth of prognostic information available for management of patients with ischemic heart disease based on stratification by FPRNA exercise LVEFs (5,7,9). Despite these advantages, widespread use of FPRNA has been limited by the need for large-bore intravenous access (23), impeccable bolus technique (32), and a high-count rate capable, often dedicated, gamma camera. It has further been impeded by published data indicating that FPRNA LVEFs cannot be substituted for those obtained with GERNA or contrast ventriculography (14,22,24–26).

It has been shown by other imaging techniques, including echocardiography and MRI (28–31), that the base of the heart,

including the aortic valve plane, moves toward the apex during systole. The extent of this motion is an index of systolic function. In patients with a normal LVEF, the descent of the base of the heart exceeds 10 mm (29). Thus, the standard method of FPRNA analysis with a fixed ROI drawn, end-diastolic ROI is likely to have substantial contamination from the end-systolic counts within the aortic root and sinuses of Valsalva. Using a single ROI drawn at end-systole would exclude the counts in the basal portion of the ventricle at end-diastole. Both of these types of errors would result in a lowering of the EF.

The dual-ROI correction for valve plane motion taken in this study is similar to that used at many centers using the recent versions of commercially available software for the SIM-400 (Picker International, Cleveland, OH). This correction resulted in a mean increase of 0.06 in LVEF measurements (i.e., 6 EF units, a 13% increase), to a range of values that was equivalent to that obtained with GERNA, a technique that similarly uses a variable ROI analysis. This increase in the measured EF should be applicable to any scintigraphic device that uses a single ROI throughout the cardiac cycle.

An automated selection of valve planes and ROIs would be preferable in order to eliminate subjectivity from the measure-

ment. However, due to the inherent objectivity provided by the Fourier amplitude images, these results demonstrated a high degree of inter- and intraobserver reproducibility.

CONCLUSION

Despite good correlation between the techniques, the standard single-ROI method of FPRNA significantly underestimates the LVEFs of GERNA, as well as the LVEFs of other imaging methods (*14,22,24–26*). This can be eliminated by accounting for valve plane motion during the cardiac cycle using Fourier-guided, dual-ROI analysis of FPRNA, giving LVEFs that are highly reproducible and similar in value to GERNA.

REFERENCES

1. Greenberg H, McMaster P, Dwyer EM, Multicenter Postinfarction Research Group. Left ventricular dysfunction after acute myocardial infarction: the results of a prospective multicenter study. *J Am Coll Cardiol* 1984;4:867–874.
2. Nesto RW, Cohn LH, Collins JJ Jr, Wynne J, Holman L, Cohn PF. Inotropic contractile reserve: a useful predictor of increased 5 year survival and improved post-operative left ventricular function in patients with coronary artery disease and reduced ejection fraction. *Am J Cardiol* 1982;50:39–44.
3. Ritchie JL, Hallstrom AP, Troubaugh GB, Caldwell JH, Cobb LA. Out-of-hospital sudden coronary death: rest and exercise left ventricular function in survivors. *Am J Cardiol* 1985;55:645–651.
4. Williams KA, Sherwood DF, Fisher KM. The frequency of asymptomatic and electrically silent exercise-induced regional myocardial ischemia during first-pass radionuclide angiography with upright bicycle ergometry. *J Nucl Med* 1992;33:359–364.
5. Lee KL, Pryor DB, Pieper KS, et al. Prognostic value of radionuclide angiography in medically treated patients with coronary artery disease. a comparison with clinical and catheterization variables. *Circulation* 1990;82:1705–1717.
6. Muhlbaier LH, Pryor DB, Rankin JS, et al. Observational comparison of event-free survival with medical and surgical therapy in patients with coronary artery disease. 20 years of follow-up. *Circulation* 1992;86(suppl 5):II198–204.
7. Jones RH, Johnson SH, Bigelow C, et al. Exercise radionuclide angiocardiography predicts cardiac death in patients with coronary artery disease. *Circulation* 1991; 84(suppl 3):152–58.
8. Johnson SH, Bigelow C, Lee KL, Pryor DB, Jones RH. Prediction of death and myocardial infarction by radionuclide angiocardiography in patients with suspected coronary artery disease. *Am J Cardiol* 1991;67:919–26.
9. Pryor DB, Harrell FE Jr, Lee KL, et al. Prognostic indicators from radionuclide angiography in medically treated patients with coronary artery disease. *Am J Cardiol* 1984;53:18–22.
10. Zhu WX, Gibbons RJ, Bailey KR, Gersh BJ. Predischard exercise radionuclide angiography in predicting multivessel coronary artery disease and subsequent cardiac events after thrombolytic therapy for acute myocardial infarction. *Am J Cardiol* 1994;74:554–559.
11. Jones RH, Borges-Neto S, Potts JM. Simultaneous measurement of myocardial perfusion and ventricular function during exercise from a single injection of ^{99m}Tc-sestamibi in coronary artery disease. *Am J Cardiol* 1990;66:68E–71E.
12. Berman DS, Kiat H, Maddahi J. The new ^{99m}Tc myocardial perfusion imaging agents: ^{99m}Tc-sestamibi and ^{99m}Tc-teboroxime. *Circulation* 1991;84(suppl 3):17–21.
13. Williams KA, Taillon LA, Draho JM, Foisy MF. First-pass radionuclide angiographic studies of left ventricular function with ^{99m}Tc-teboroxime, ^{99m}Tc-sestamibi and ^{99m}Tc-DTPA. *J Nucl Med* 1993;35:394–399.
14. Williams KA, Taillon LA. Gated planar technetium-99m-sestamibi myocardial perfusion image inversion for quantitative scintigraphic assessment of left ventricular function. *J Nucl Cardiol* 1995;2:285–295.
15. Baillet GY, Mena IG, Kuperus JH, Robertson JM, French WJ. Simultaneous technetium-99m-MIBI angiography and myocardial perfusion imaging. *J Nucl Med* 1989;30:38–44.
16. Larock MP, Cantineau R, Legrand V, Kulbertus H, Rigo P. Technetium-99m-MIBI (RP-30) to define the extent of myocardial ischemia and evaluate ventricular function. *Eur J Nucl Med* 1990;16:223–230.
17. Elliott AT, McKillop JH, Pringle SD, et al. Simultaneous measurement of left ventricular function and perfusion. *Eur J Nucl Med* 1990;17:310–314.
18. Villanueva-Meyer J, Mena I, Narahara KA. Simultaneous assessment of left ventricular wall motion and myocardial perfusion with technetium-99m-methoxy isobutyl isonitrile at stress and rest in patients with angina: comparison with thallium-201 SPECT. *J Nucl Med* 1990;31:457–463.
19. Sporn V, Perez-Balino N, Holman BL, et al. Simultaneous measurement of ventricular function and myocardial perfusion using the technetium-99m isonitriles. *Clin Nucl Med* 1988;13:77–81.
20. Bisi G, Sciagra R, Bull U, et al. Assessment of ventricular function with first-pass radionuclide angiography using technetium-99m hexakis-2-methoxyisobutylisonitrile: a European multicentre study. *Eur J Nucl Med* 1991;18:178–183.
21. Boucher CA, Wackers FJ, Zaret BL, Mena IG. Technetium-99m-sestamibi myocardial imaging at rest for assessment of myocardial infarction and first-pass ejection fraction. Multicenter Cardiolite Study Group. *Am J Cardiol* 1992;69:22-2-7.
22. Williams KA, Taillon LA. Left ventricular function in patients with coronary artery disease using gated tomographic myocardial perfusion images: comparison with contrast ventriculography and first-pass radionuclide angiography. *J Am Coll Cardiol* 1996;27:173–181.
23. Williams KA, Walley PE, Ryan JW. Detection and assessment of severity of tricuspid regurgitation using first-pass radionuclide angiography and comparison with pulsed Doppler echocardiography. *Am J Cardiol* 1990;66:333–339.
24. Nusynowitz ML, Benedetto AR, Walsh RA, Starling MR. First-pass anger camera radiocardiography: biventricular ejection fraction, flow and volume measurements. *J Nucl Med* 1987;28:950–959.
25. Folland ED, Hamilton GW, Larson SM, Kennedy JW, Williams DL, Ritchie JL. The radionuclide ejection fraction: a comparison of three radionuclide techniques with contrast angiography. *J Nucl Med* 1977;18:1159–1166.
26. Nichols K, DePuey EG, Gooneratne N, Salensky H, Friedman M, Cochoff S. First-pass ventricular ejection fraction using a single-crystal nuclear camera. *J Nucl Med* 1994;35:1301–1302.
27. Vainio P, Jurvelin J, Kuikka J, Vanninen E, Lansimies E. Analysis of left ventricular function from gated first-pass and multiple gated equilibrium acquisitions. *Int J Card Imaging* 1992;8:243–247.
28. Simonson J, Schiller N. Decent of the base of the left ventricle: an echocardiographic index of left ventricular function. *J Am Soc Echocardiogr* 1989;2:25–35.
29. Alam M, Rosenhamer G. Atrioventricular plane displacement and left ventricular function. *J Am Soc Echocardiogr* 1992;5:427–433.
30. Arts T, Hunter WC, Douglas AS, Muijtjens AM, Corsel JW, Reneman RS. Macroscopic three-dimensional motion patterns of the left ventricle. *Adv Exper Med Biol* 1993;346:383–392.
31. Qi P, Thomsen C Stahlberg F, Henriksen O. Normal left ventricular wall motion measured with two-dimensional myocardial tagging. *Acta Radiologica* 1993;34:450–456.
32. Gal R, Grenier RP, Carpenter J, Schmidt DH, Port SC. High count rate first-pass radionuclide angiography using a digital gamma camera. *J Nucl Med* 1986;27:198–206.
33. Gal R, Grenier RP, Schmidt DH, Port SC. Background correction in first-pass radionuclide angiography: comparison of several approaches. *J Nucl Med* 1986;27:1480–1486.
34. Zar JH. *Biostatistical analysis*, 2nd ed. Englewood Cliffs, NJ: Prentice-Hall; 1984: 316–317.
35. Bland JM, Altman DG. Statistical methods for assessing agreement between two methods of clinical measurement. *Lancet* 1986;1:307–310.
36. Bland JM, Altman DG. A note on the use of the intraclass correlation coefficient in the evaluation of agreement between two methods of measurement. *Comput Biol Med* 1990;20:337–340.